# An Intercomparison of ERS-Scat and AMSR-E Soil Moisture Observations with Model Simulations over France

Christoph Rüdiger, Jean-Christophe Calvet, Claire Gruhier, R.H. Holmes
Thomas, A.M. de Jeu Richard, Wolfgang Wagner

## HAL Id: ird-00394903
## https://hal.ird.fr/ird-00394903

Submitted on 23 Jul 2009

# An Intercomparison of ERS-Scat and AMSR-E Soil Moisture Observations with Model Simulations over France

Christoph Rüdiger[1,*]
Jean-Christophe Calvet[1]
Claire Gruhier[2]
Thomas Holmes[3]
Richard de Jeu[3]
Wolfgang Wagner[4]


[1]CNRM-GAME, Météo-France/CNRS, France
[2]CESBIO, UMR5126 CNES/CNRS/IRD/UPS, France
[3]Faculty of Earth and Life Sciences, Vrije Universiteit Amsterdam, Netherlands
[4]Institute of Photogrammetry and Remote Sensing, Vienna University of Technology, Austria

* now at: Department of Civil and Environmental Engineering, The University of Melbourne, Australia

CORRESPONDING AUTHOR:

Jean-Christophe Calvet

Météo-France
CNRM/GMME/MC2
Toulouse, France

Phone: +33 5 6107 9341
Fax: +33 5 6107 9626
Email:
calvet@meteo.fr

1    **Abstract**

2    This paper presents a study undertaken in preparation of the work leading up to the

3    assimilation of SMOS observations into the land surface model (LSM) ISBA at Météo

4    France. This study consists of an inter-comparison experiment of different space-borne

5    platforms providing surface soil moisture information (AMSR-E and ERS-Scat) with the

6    reanalysis soil moisture predictions over France from the model suite SIM (SAFRAN-ISBA-

7    MODCOU) of Météo France for the years 2003 to 2005. Both modelled and remotely sensed

8    data are initially validated against in-situ observations obtained at the experimental soil

9    moisture monitoring site SMOSREX in south-western France. Two different AMSR-E soil

10    moisture products are compared in the course of this study (the official AMSR-E product

11    from the National Snow and Ice Data Centre (NSIDC) and a new product developed at the

12    Vrije Universiteit Amsterdam and NASA (VUA-NASA)), which were obtained using two

13    different retrieval algorithms. This allows an additional assessment of the different

14    algorithms, while using identical brightness temperature data sets. This study shows that a

15    good correlation exists between AMSR-E (VUA-NASA), ERS-Scat, and SIM, generally for

16    low altitudes and low-to-moderate vegetation covers (1.5 to 3kg m² vegetation water content),

17    with a reduction in the correlation in mountainous regions. It is also shown that the AMSR-E

18    (NSIDC) soil moisture product has significant differences, when compared to the other data

19    sets.

20

21

22

## 1. Introduction

Soil moisture is the governing variable for modelling soil surface-to-atmosphere energy exchanges and land surface model (LSM) initialisation, as it controls both evaporation and transpiration from bare soil surfaces and vegetation covers. Consequently, a significant amount of studies have been and are currently being conducted to obtain soil moisture estimates through land surface modelling (e.g. Dirmeyer et al. 1999; Georgakakos and Carpenter 2006) and remotely sensed surface soil moisture observations (e.g. Wagner et al. 1999ab; Kerr et al. 2001; Njoku et al. 2003).

For the purpose of soil moisture remote sensing, observations in the microwave bands have been found to produce the best results. The optimal wavelength lies within the L-band range (~1-2GHz), as interference through vegetation water content at this frequency range is lower than at higher frequencies.. However, instruments have in the past been and are currently operated at higher frequencies (above 5GHz), mainly because none of these missions were dedicated soil moisture missions. The first such dedicated soil moisture mission will be the Soil Moisture and Ocean Salinity mission (SMOS), to be launched in 2009. The first microwave instrument operated for an extensive time and within adequate wavelengths was the Scanning Multichannel Microwave Radiometer (SMMR) on Nimbus-7 (operational from 1978 to 1987), which operated at bands at and above 6.6GHz. SMMR was followed by the Special Sensor Microwave/Imager (SSM/I; since 1987) and the similar Tropical Rainfall Measuring Mission (TRMM) Microwave Imager (TMI; since 1997), which operate at frequencies above 10GHz. Instruments which are currently operational at frequencies similar to SMMR (and therefore closer to L-band), are the Advanced Microwave Scanning Radiometer for the Earth Observing System (AMSR-E) on board NASA's Aqua satellite, WindSat on board the American Navy's Coriolis satellite, and the scatterometers on board the European Remote Sensing satellites (ERS-1 & -2). Finally, a new scatterometer

47   (ASCAT) was launched on board ESA's MetOp satellite in 2006 and its data will soon be

48   available operationally (Bartalis et al. 2007).

49       Despite almost 30 years of experience with these microwave remote sensing instruments,

50   it is still necessary to validate the soil moisture products obtained from these instruments

51   through in-situ soil moisture observations. However, such ground-truthing has only been

52   achieved over small temporal and spatial scales (eg. the Soil Moisture Experiments (SMEX)

53   or the Campaign for validating the Operation of SMOS (CoSMOS)), as it is economically and

54   practically infeasible to observe soil moisture at high spatial and temporal resolution over

55   large scales using in-situ observations, mainly because of its high spatial variability.  Only in

56   the present decade there have been attempts to establish long-term and large scale soil

57   moisture observation networks or data banks such as the Global Soil Moisture Data Bank

58   (Robock et al. 2000), the Goulburn River experimental catchment in Australia (Rüdiger et al.

59   2007), or SMOSMANIA in south-western France (Calvet et al. 2005). However, these data

60   sets only represent single points in space. This lack of spatial extent limits the usefulness of

61   such data sets for assimilation into large scale land surface models and also for disaggregation

62   studies, as the large scale, but also subpixel variability is not captured with single point

63   measurements. Moreover, satellite products are generally available at scales of about 0.25° or

64   25km, which leads to problems in their validation process, due to the different spatial scales

65   (spatially averaged satellite products are compared to point measurements). Consequently,

66   new validation methods complementing the existing soil moisture networks have to be

67   conceived (Wagner et al. 2007). Under the assumption that LSMs, forced with high quality

68   atmospheric forcing data, adequately represent the surface soil moisture dynamics, the scale

69   issues can be reduced. This assumption in turn will then allow the large-scale and long-term

70   evaluation of the satellite products in terms of their temporal dynamics, as the products

71   considered are essentially independent models.

4

72       In this paper, both the need for large scale ground-truthing and understanding of the

73       subpixel heterogeneity of soil moisture are addressed. First, the temporal correlation of

74       satellite products at a large scale with a synthetic high-resolution surface soil moisture data

75       base is presented. The high-resolution meteorological observation network throughout France

76       (more than 1000 surface meteorological stations and more than 3500 daily rain gauges) has

77       resulted in a high-quality atmospheric forcing data base (Quintana-Seguí et al. 2008) for the

78       operational land surface model ISBA of Météo-France, within the modelling system SIM

79       (SAFRAN-ISBA-MODCOU; Habets et al., 2008). The SIM model simulates the soil moisture

80       dynamics.

81       The satellite products used for this study were obtained from AMSR-E and ERS-2.

82       Furthermore, the recent development of a new retrieval algorithm for AMSR-E (Owe et al.

83       2007) allowed to compare the official AMSR-E product (Njoku et al. 2003) with this new

84       data base. In the first part of this study, the different data sets used are discussed, followed by

85       a brief comparison of those remotely sensed data sets and SIM with in-situ observations of the

86       SMOSREX experimental site near Toulouse, France (de Rosnay et al. 2006), to determine

87       their capability to represent the temporal soil moisture dynamics of a point or pixel. The good

88       results of this analysis between the land surface model, in-situ observations, and satellite data

89       also shows that previous results obtained over Spain (Wagner et al. 2007; one single satellite

90       pixel), or over Australia (Draper et al. 2007; several in-situ observations for a number of

91       pixels) can be extrapolated to a national or even continental scale, as they show the same

92       tendencies. The differences between the various soil type data bases used in the satellite

93       retrieval schemes and the model data base, make it difficult to compare absolute values.

94       Consequently, the discussion of this paper will focus on the normalised data sets. In the

95       second part, the inter-comparison study then presents the correlations and mean differences

96       between all data sets (ie. also between the different satellite products).

97

## 2. Data Sets

99    Due to the limitation in the spatial extent of SIM, this study is limited to watersheds of

100  mainland France. Nevertheless, the surface and climatic conditions throughout the country are

101  sufficiently variable (ranging from sub-humid to alpine), to give a statistically sound data

102  basis for a representative analysis. The years 2003-2005 were chosen for this study, as data

103  exists for all sources (SIM – 1970 to 2006; ERS-Scat – 1992 to 2006; AMSR-E – 2003 to

104  date; and SMOSREX – 2001 to date). Moreover, this 3-year period includes both very dry

105  and very wet climatic conditions, which are necessary to determine the dynamic range of the

106  soil moisture observations within each pixel. The following sections briefly outline the

107  various data sets, used for this study.

108

109        *a. SAFRAN-ISBA-MODCOU (SIM)*

110  The modelled surface soil moisture data base was obtained from the modelling system

111  SAFRAN-ISBA-MODCOU (SAFRAN – atmospheric forcing data base; ISBA – land surface

112  model; MODCOU – hydrological routing model). Of these three model chain segments, only

113  SAFRAN and ISBA were of importance for the present study.

114  SAFRAN (Système d'analyse fournissant des renseignements atmosphériques pour la

115  nivologie) is a reanalysis forcing data base, initially developed to improve snowfall and

116  avalanche forecasting. Within SAFRAN, the main atmospheric forcing parameters are

117  analysed. Each atmospheric parameter is analysed individually using an optimal interpolation

118  method. The final size of a grid cell within SAFRAN is 8x8 km$^2$. For precipitation, however,

119  the actual pixel sizes of SAFRAN vary, as they represent zones of climatic conditions rather

120  than regularly gridded areas. Each climatic zone covers about 1000km², resulting in about 600

121  such pixels over France. The forcing parameters are in principle assumed to be homogeneous

122  within one such pixel, however, they vary on a sub-pixel scale with topography. Apart from

123  precipitation the SAFRAN forcing data is available at 6-hourly intervals. Precipitation is

124  obtained using daily observations at the rain gauges and then interpolated into hourly time

125  steps as a function of the relative humidity during the day. The SAFRAN data base has

126  recently been validated against in-situ observations and found to be well correlated (Quintana-

127  Seguí et al. 2008).

128      The land surface model used in SIM is ISBA (Interactions of the Soil, Biosphere and

129  Atmosphere; Noilhan and Planton 1989; Mahfouf and Noilhan 1996), which is used

130  operationally as the land surface scheme within the numerical weather prediction system at

131  Météo-France. The soil layer and soil moisture dynamics are modelled within a 3-soil-layer

132  model (Boone et al. 1999), which is based on the force-restore approach, where the three soil

133  layers are a surface layer of 1cm depth, forming part of a root zone layer above the third, deep

134  layer.

135      There is no previous study presenting a verification of the SIM surface soil moisture

136  product. On the other hand, the ISBA model has been extensively validated for various

137  biomes. In particular, a number of studies exist comparing a point-specific calibrated ISBA

138  version to actual in-situ soil moisture observations in France (Calvet et al. 1998a,b, Boone et

139  al. 1999, Calvet and Noilhan 2000, and Sabater et al. 2007). The latter case corresponds to

140  SMOSREX, and the former to a previous experiment (MUREX) in the same region. The

141  RMSE for those cases is, respectively, 0.06 and 0.07 $m^3m^{-3}$, with a mean difference in the

142  order of 0.01 and 0.03 $m^3m^{-3}$. In both cases the Nash efficiency was calculated with 0.65/0.59.

143  Based on the results of Prigent et al. (2005), this level of error between in-situ observations

144  and model predictions is expected, while maintaining a good correlation despite the different

145  observation and model layer depths. The land surface parameters for ISBA are obtained from

7

146  ECOCLIMAP (Masson et al. 2003). The parameters provided by ECOCLIMAP are originally

147  provided at 1km resolution and are aggregated to the model resolution of 8km.

148

149      *b.  AMSR-E*

150      AMSR-E is a passive microwave scanning radiometer, operating at six wavelengths

151  within the microwave spectrum (6.925, 10.65, 18.7, 23.8, 36.5, and 89GHz) in horizontal and

152  vertical polarisations, flown on NASA's Aqua satellite. The total swath width during an

153  overpass is approximately 1445km, with footprint resolutions ranging from 56km (6.925GHz)

154  to 5km (89GHz). Aqua is a sun-synchronous satellite orbiting Earth approximately 14 times

155  each day, with morning/descending and afternoon/ascending overpasses, at around

156  1.30am/pm. This configuration results in a repeat coverage of approximately every three days

157  in the equatorial latitudes and more frequent coverage in higher latitudes. For the particular

158  case of France, Aqua overpasses take place at 4 out of 5 days for both ascending and

159  descending orbits.

160      Currently, two different data products are freely available. The official product can be

161  obtained through the National Snow and Ice Data Center (NSIDC, hereafter AMSR-E

162  (NSIDC)), while a new product has recently been made available through the Vrije

163  Universiteit Amsterdam in collaboration with NASA (hereafter AMSR-E (VUA-NASA)).

164  Both products are briefly described in the following sections.

165          i.      AMSR-E (NSIDC)

166      The AMSR-E (NSIDC) data used for this study were obtained from the operational Level

167  3 B03 AMSR-E data set (Njoku 2006). While the original resolution at 10.65GHz is ~38km,

168  the data is binned into regular 0.25°x0.25° pixels, through oversampling at 10km intervals.

8

169    The NSIDC method uses two low frequency dual polarized channels to optimize the three

170    parameters (soil moisture, vegetation optical depth and the effective soil temperature)

171    simultaneously. Originally, the method was developed and tested for the C- and X- band

172    channels. Unfortunately, severe radio-frequency interference (RFI) was discovered within C-

173    band (6.925GHz) over the USA and Japan and X-band over Italy and Great Britain  (Li et al

174    2004, 2006). For this reason, the retrieval algorithm was applied to the X-band (10.65GHz)

175    and Ku-band (18.7 GHz) brightness temperatures. This has some important disadvantages: 1)

176    the 18 GHz channel introduces atmospheric influences and, 2) the observation depth of the

177    soil moisture product is reduced to 5-10mm, which is approximately half the potential range

178    of C-band and 3) vegetation attenuation effects are more significant than at lower frequencies.

179            ii.    AMSR-E (VUA-NASA)

180    The VUA-NASA retrieval products from AMSR-E are derived according to the Land

181    Surface Parameter Model (LPRM) (Owe et al. 2007). The LPRM is a three-parameter

182    retrieval model for passive microwave data, using one dual polarized channel (either 6.925 or

183    10.65GHz) for the retrieval of both surface soil moisture and vegetation water content

184    (VWC). The land surface temperature is derived separately from the vertically polarized

185    36.5GHz channel.

186    The forward radiative transfer model in LPRM is based on one vegetation layer ($\tau$-$\omega$

187    approach) and the vegetation optical depth is parameterized as a function of the Microwave

188    Polarization Difference Index (MPDI) and soil moisture according to Meesters et al. (2005).

189    This method is applied globally, and requires no regional calibration or fitting parameters to

190    aid the retrieval process.

191    The main differences with the AMSR-E (NSIDC) soil moisture product lies in the use of

192    a higher frequency band for the retrieval of the land surface temperature (LST), and the

193  parameterization of the vegetation optical depth, leaving only the soil moisture to be

194  optimized.

195

196      *c.  ERS-Scat*

197      The ERS-Scat data is obtained through active microwave remote sensing, ie. an energy

198  pulse is sent to the surface and the intensity of the returned signal is then used within the

199  retrieval algorithm to derive a relative soil moisture state. ERS-Scat is operated at 5.3GHz (C-

200  band), observing only the vertically polarised backscatter within this band, thus resulting in a

201  similar observation depth as AMSR-E. RFI has been found to have little impact on active

202  microwave remote sensing at this frequency. ERS-Scat has a morning/descending and

203  evening/ascending orbit at 10.30am/pm, with a varying repeat coverage of about 2 to 8 days.

204  The spatial resolution of an ERS-Scat footprint is in the order of 50km, while the soil

205  moisture product is binned into pixels of 0.25° (north-south extent) and 25km (west-east

206  extent).

207      The soil moisture product is provided in relative values, ranging from 0 to 100%. The

208  normalisation of the backscatter signal is done, using the minimum and maximum observed

209  backscatter from the 1992-2000 period, as dry and wet references. The retrieval algorithm is

210  described in detail in Wagner et al. (1999, 2003).

211      *d.  SMOSREX*

212      SMOSREX is an experimental field site for in-situ and remotely sensed soil moisture

213  observations jointly operated by various research institutes in France and located to the south

214  of Toulouse (43°23'N, 1°17'E) in south-western France (De Rosnay et al. 2006). The overall

215  size of SMOSREX is approximately 6000m² separated into two areas with either bare soil or

216  fallow. The climate is temperate with monthly mean maximum temperatures of 5°C in winter

217    and 24°C in summer and an average annual cumulative precipitation of about 650mm. The

218    surface soil consists of a sandy loam, with 16% clay, 47% silt, and 37% sand.

219        Most instruments installed at the site have been in operation since 2001. The main feature

220    of this site is a tower-mounted L-band radiometer for the production of multi-angle brightness

221    temperatures. Other instrumentation include a weather station, and soil temperature and

222    moisture sensors, installed at various points and depths. The soil moisture sensors (Theta

223    Probes ©) used for this study are located at four points within the fallow section of the site

224    (most representative for the overall region and therefore the model simulations), with a

225    spacing of only a few metres. The sensors are vertically inserted at the surface, therefore

226    integrating the soil moisture content from 0 to 6cm, and a temporally averaged soil moisture

227    content is stored every 30 minutes individually for all sensors. The calibration of the sensors

228    is presented in (De Rosnay et al. 2006).

229        For the purpose of this study, the in-situ observations were aggregated into daily averages

230    and compared to the respective data sets obtained through the model and remote sensing.

231    Spatially averaging the observations of those four probes reduces the effect of spatial

232    variability within and increases the representativity of the soil moisture observations, and also

233    reduces the individual observations to one point in space.

234

235        *e.  Data Preparation*

236        The results presented in this paper are based solely on the data sets from descending

237    orbits (nighttime) to avoid overly solar effects in the satellite data, due to sun glint and strong

238    temperature gradients between the vegetation and the surface, and also within the surface

239    layer, but also due to Faraday rotation and temperature gradients within the sensor which are

240    more pronounced during daytime overpasses (Kerr and Njoku 1990). Other effects such as

241   quick dry-down or the lack thereof due to local changes in solar radiation, which can not be

242   adequately represented in an LSM and in reality may be affected by cloud coverage and wind,

243   among other factors play a significant role in the daytime evolution of surface soil moisture.

244   While the in-situ observations were spatially and temporally averaged, the soil moisture

245   simulations were extracted for the time steps close to the overpass times of the satellites. A

246   comparison of the differences between the individual measurements of the soil moisture

247   probes and their spatial average at 6am and also between the daily average with the spatial

248   average at 6am resulted in an RMSE of 0.036 $m^3m^{-3}$ in both cases. This shows that spatial and

249   diurnal variabilities contribute to the same extent to the uncertainty in the in-situ observations.

250   The use of a spatially and temporally daily average is therefore justifiable.

251       All data have been reprojected from their original coordinate systems onto a regular

252   0.25°x0.25° grid using a nearest neighbour approach. As the overall footprints of AMSR-E

253   and ERS-Scat are in the order of 50km with a spacing of about 10km between the centre

254   points, and the gridded products used in this study are binned at 25km or 0.25°, respectively, a

255   spatial shift in the data due to the reprojection process (a maximum of 12km) is not expected

256   to add any additional noise to the data or affect the data quality, as a footprint with its centre

257   12km from the pixel centre would still include information from more than half of the land

258   surface corresponding to the pixel area due to its size. To obtain an average pixel value within

259   the reprojected pixels, all original pixels with their centre falling into one reprojected pixel

260   were averaged to one single value. This average value was then assumed to be the

261   representative soil moisture of the reprojected pixel. In the case of the satellite observations,

262   only one original pixel would generally fall into a reprojected pixel, due to the similarity in

263   size, so that no errors are introduced due to the averaging of two satellite pixels. For all data

264   sets, the same general rule applied for the reprojection process, to avoid inconsistencies

265   between the data sets introduced through the reprojection and aggregation process.

266    In a brief study it was examined whether the variability between the soil moisture of high

267    resolution SIM pixels with their averaged low resolution equivalent resulted in any errors

268    within the analysis. However, no relationship between the this subpixel heterogeneity and the

269    spatial distribution of the correlation coefficients between the different soil moisture products

270    presented in the following section was found.

271    The soil moisture data from the satellites and SMOSREX were normalised following the

272    approach presented by Pellarin et al. (2006), where the maximum and minimum of the soil

273    moisture range was not determined by the soil type, but rather by the observed dynamic range

274    within each individual pixel within the full study period (2003-2005). To exclude any

275    abnormal outliers due to observational errors or instrument noise, the 90% confidence interval

276    was chosen to define the upper and lower soil moisture content, respectively, using (1) and

277    (2).

278    $$int^+(SM) = \mu(SM) + 1.64 * \sigma(SM) \qquad\qquad (1)$$

279    and

280    $$int^-(SM) = \mu(SM) - 1.64 * \sigma(SM) \qquad\qquad (2)$$

281    where $int^+$ and $int^-$ are the upper and lower confidence limits; $\mu(SM)$ is the average soil

282    moisture content for the pixel; and $\sigma(SM)$ the standard deviation of the soil moisture content

283    for each pixel.  With the knowledge of the upper and lower soil moisture content the absolute

284    soil moisture value is then normalised using (3):

285    $$\theta_n = \frac{SM_{obs} - int^-}{int^+ - int^-} \qquad\qquad (3)$$

286    where $SM_{obs}$ is the individual soil moisture observation and $\theta_n$ is its normalised soil moisture

287    value. As a simplification it is assumed that the data are normally distributed, so that 90% of

288    the data lie by definition within a range of $\mu \pm 1.64\sigma$. All data outside of this range were

289    discarded. Also, pixel values were excluded from the overall analysis, where SIM predicted

290    frozen soil water. As model simulations as such have no outliers due to instrumentation

291    errors, no screening of extreme values is required. The soil moisture from SIM is therefore

292    normalised using the modelled maxima and minima of each individual pixel, instead of $int^+$

293    and $int^-$.

294        Pixels located over major urban agglomerations (ie. Lille, Paris, Lyon, Bordeaux,

295    Toulouse, and Marseille) were not excluded. However, the correct representation of the soil

296    moisture is doubtful, as SIM is not capable to give realistic soil moisture conditions over

297    urban (and consequently sealed) areas, and moreover, the possibility of pixels subjected to

298    potential radio-frequency interference (Li et al. 2004) is higher in these areas. Nevertheless,

299    the number of these pixels is small (<0.5% of the total), compared to the total over France and

300    their overall effect on the statistical analyses was found to be negligible.

301

302    **3. Comparison of the soil moisture products with in-situ observations**

303        An evaluation of the surface soil moisture products obtained from SIM and the satellites

304    was undertaken, using the same three years of in-situ soil moisture observations as for the

305    remainder of this study (2003-2005). The in-situ data were obtained from the observations at

306    the experimental site SMOSREX. The data from the four surface soil moisture sensors

307    installed at SMOSREX, were averaged both spatially and over time, so that one daily

308    averaged observation was obtained for each day. This approach reduced the existing noise

309    levels in the in-situ observations, as discussed in the previous section. The model and satellite

310    data used here are the binned and reprojected data as for the large scale study in section 4, as

311    described above. SIM was not especially calibrated to the conditions at SMOSREX. For this

312    evaluation study various statistical parameters were calculated: the root mean square error

313 (RMSE), the mean difference or bias between two data sets, the correlation coefficient (r)

314 between two data sets, and the Nash efficiency coefficient (N). All statistics presented in the

315 following sections were calculated for the normalised soil moisture values and are therefore

316 dimensionless.

317     In a first step, the absolute values of the soil moisture products were compared with the

318 in-situ data. For this purpose, the already normalised ERS-Scat data were transferred into

319 absolute values, using the known maximum and minimum surface soil moisture observations

320 at SMOSREX. While a good correlation exists between SIM and SMOSREX data sets, a

321 severe lack of soil moisture dynamics is observed for the AMSR-E (NSIDC) data set (not

322 shown). However, the AMSR-E (VUA-NASA) data is well correlated despite an apparent wet

323 bias. Finally, the ERS-Scat observations are also well correlated in terms of their temporal

324 dynamics. In contrast to the AMSR-E (VUA-NASA) data, the ERS-Scat data exhibits a dry

325 bias. Due to the different soil moisture dynamics and biases, it is difficult to compare the

326 various data sets in detail, consequently, all comparison in the remainder of this paper will be

327 undertaken with normalised data (Fig. 1).

328     The comparison of the normalised SIM and SMOSREX data sets shows a good temporal

329 correlation (r = 0.755; N=0.478), with a bias (-0.083) towards the in-situ observations (ie. the

330 in-situ observations tend to be drier), with the exceptions of very dry conditions, when the

331 model has the tendency to overestimate the soil moisture at this site (Fig. 2). Throughout the

332 years, a higher level of surface soil moisture dynamics is observed within the model data (Fig.

333 1), which results in a root mean square error (RMSE) of 0.198. This phenomenon is explained

334 by inaccuracies in the forcing data due to the spatial interpolation process within SIM and the

335 differences in the thickness of the observed soil layers (1cm for SIM against 0-6cm for the

336 ThetaProbes). However, there are only few data points causing this noise and this is

337 consequently deemed acceptable.

338       The normalised AMSR-E (NSIDC) data display a very high variation, with interchanging

339    peaks and troughs every three months (Fig. 1). Every year, minimal values are reached during

340    winter and their maximum in summer. This recurring negative correlation with the in-situ data

341    results in a high RMSE and low overall correlation (r = 0.132; N=-0.734; bias = 0.132; RMSE

342    = 0.356). In contrast to the comparison of the absolute data, the persistent wet bias in the

343    AMSR-E (VUA-NASA) data has been reduced due to the normalisation. Similar to the SIM

344    predictions, a strong correlation between in-situ and remotely sensed data is found in this case

345    with a wet bias towards the AMSR-E data (r = 0.775; N=0.471; bias = 0.072; RMSE = 0.194).

346    Finally, the ERS-Scat observations are also well correlated over time with the in-situ data (r =

347    0.618; N=0.125), however a dry bias (-0.085) results in a more significant RMSE of 0.244

348    than for the AMSR-E (VUA-NASA) data.  As ERS-Scat data are only available from August

349    2003 onwards, the identical periods of data cover (ie. August 2003 – December 2005) for the

350    other surface soil moisture products was undertaken (not shown), in order to verify that the

351    first seven months did not introduce significant biases in the statistical analyses, which then

352    would not be seen in the ERS-Scat comparisons.  The differences in correlation, RMSE, and

353    bias did not change significantly for any of the inter-comparisons covering either the full three

354    years or the period August 2003 – December 2005.  Consequently, all comparisons shown in

355    the remainder of this paper are based on the full period. The Nash efficiency coefficient for

356    SIM and AMSR-E (VUA-NASA) are acceptable. They are also similar to each other

357    suggesting that the two data sets perform equally well compared to the in-situ observations,

358    while the low Nash efficiency of ERS-Scat is due to the relatively strong bias in the satellite

359    data. In the case of the AMSR-E (NSIDC) data, the negative Nash efficiency suggests by

360    definition that an average value of the in-situ observations would compare better with the

361    overall observations than the remotely sensed observations. This is an important finding as it

362    shows the extreme difference between the in-situ observations and the satellite product.

363    Four aspects have to be considered for the cause of the differences observed in this

364    evaluation: i) the scale difference (8km and 0.25° for the model and the satellite, respectively,

365    against a single point observation), as the comparison or validation of soil moisture products

366    at different spatial scales will remain difficult in most cases, unless a representative catchment

367    average soil moisture monitoring site (Grayson and Western 1998) can be identified; ii) the

368    soil data base, as the model soil information constitutes an average of the soil particle size

369    distribution within an 8km/0.25° pixel, which may result in significant differences compared

370    to the soil conditions at the point of observation (the particle size analysis for SMOSREX

371    yielded 16% clay, 47% silt, and 37% sand; the particle size distribution within ECOCLIMAP

372    is 25%/25%/50%), iii) the forcing data, as it is obtained by interpolation between observations

373    and atmospheric predictions, which may miss localised events, iv) the observation depth, with

374    the model layer of 1cm and approximately the same depth for the satellite observations

375    against the integrated soil moisture content at 0-6cm for the in-situ observations, may result in

376    different dynamics.

377    Considering the above four aspects, SIM, AMSR-E (VUA-NASA) and ERS-Scat perform

378    well when compared to the SMOSREX in-situ observations, and also show a good

379    representation of the dynamic behaviour of the soil moisture content. For SIM, an RMSE of

380    0.198 with a dynamic range of the surface soil moisture at the site of ~0.3 $m^3m^{-3}$, can be

381    translated into an absolute error in the soil moisture of just under 0.06 $m^3m^{-3}$. This result is

382    particularly good, as SIM was not calibrated to the conditions at SMOSREX, but rather used

383    the vegetation and soil conditions obtained from ECOCLIMAP. Moreover, despite the

384    differences in scale these errors are identical to the performance of the site-specific calibrated

385    model.

386    Depending on the application, the calculated error may be considered large or acceptable.

387    For atmospheric studies, it is more important to obtain a good representation of the temporal

388    dynamics, while the absolute soil moisture state is less important. On the other hand, an error

389    of 0.06 m$^3$m$^{-3}$ exceeds the validation goals of future satellite missions (Kerr et al, 2001). In

390    the first case, the evaluation of satellite data against any benchmark is necessary, shown by

391    the lack of temporal dynamics in the AMSR-E (NSIDC) data. In the second case, two factors

392    influencing the RMSE have to be considered to qualify the above value of 0.06 m$^3$m$^{-3}$: i) the

393    mean difference or bias between SIM and SMOSREX and ii) the spatial uncertainty of the in-

394    situ observation. Biases, in the case of the normalised data 0.084 (or 0.025 m$^3$m$^{-3}$), may be

395    removed using various techniques (eg. Drusch et al., 2005), while the uncertainty in the

396    spatial averaging of the four in-situ observations is in the order of 0.036 m$^3$m$^{-3}$. In particular

397    the removal of the bias would lead to a significant decrease of the RMSE. Consequently, it is

398    concluded that SIM may be used with reasonable confidence for a large scale model

399    intercomparison study, assuming that ECOCLIMAP provides similarly good information for

400    all other model pixels.

401    While the correlations derived from Fig. 1 are relatively large for SIM, AMSR-E (VUA-

402    NASA) and ERS-Scat, much of the captured variability is seasonal (dry in summer, wet in

403    winter). In order to assess the coherence with the in-situ observations and to avoid seasonal

404    effects, monthly anomalies are calculated. The difference to the mean is calculated for a

405    sliding window of five weeks, and the difference is scaled to the standard deviation. Table 1

406    shows seasonal scores, including the Kendall statistics and p-value. All the products are

407    significantly correlated to the in-situ observations, except for satellite products at specific

408    periods of the year. While SIM presents significant correlations throughout the year, all the

409    satellite products are not significantly correlated to in-situ observations at wintertime (DJF).

410    This may be explained by the sensitivity of the microwave signal (either active or passive) to

411    soil freezing and by the reduced dynamics of the surface soil moisture at wintertime. Both

412    VUA-NASA and NSIDC products present high correlations of the anomalies for the other

413    seasons. On the other hand, ERS-Scat has significant correlations at springtime (MAM), only.

414    The lack of significance of ERS-Scat during the summer and autumn seasons (JJA and SON,

415    respectively), may be explained by the small number of observations over the SMOSREX site

416    (28 and 41, respectively), compared with AMSR-E (184 and 175, respectively, for the VUA-

417    NASA product).

418

419

420

421

422

423    **4. Inter-Comparison (all Data Sets)**

424        *a. General Correlation (all data)*

425        Fig. 3 shows correlation maps of the different remote sensing and modelled data sets for

426    all surface conditions and all years. A good correlation exists between the three data sets

427    AMSR-E (VUA-NASA), ERS-Scat, and SIM, in particular for regions of herbaceous

428    vegetation over regions with little relief, with a range of the coefficient of correlation from 0.2

429    to 0.9. Areas with denser vegetation, such as the forest of Les Landes in the South-West along

430    the Atlantic coast show a lower level of correlation, which would have to be expected due to

431    the masking effect on the microwave emissions of the soil moisture through vegetation.

432    Similarly, low correlations are found in regions with strong relief such as the Massif Central

433    and the Alps. The good correlation of ERS-Scat with SIM in the Italian Alps should be

434    ignored, as only a few data points were available due to the overpass rate of ERS over the

435    region and the filtering of days with frozen soils or snow. Mountainous regions cause errors in

436    both the modelling of soil moisture and its retrieval from satellite observations. First, there

19

437     exists a high level of uncertainty in the soil depth and its variability in those regions, which

438     impacts on the predictions of the soil moisture dynamics in the SIM model. Secondly, relief

439     interferes with the retrieval of low resolution remotely sensed soil moisture observations and

440     may cause considerable levels of errors (Mätzler and Standley 2000). The AMSR-E (NSIDC)

441     product has virtually only low correlations with any of the other data sets, even producing

442     negative correlations overall (Table 2).

443     This analysis also shows that previous results obtained over Spain (Wagner et al. 2007;

444     one single satellite pixel), or over Australia (Draper et al. 2007; several in-situ observations

445     for a number of pixels) can be extrapolated to a national or even continental scale, as they

446     show the same tendencies. In particular, the lack of soil moisture dynamics within the AMSR-

447     E (NSIDC) data set are apparent and are shown in all studies.

448     The data used to derive the spatial plots of Fig. 3 are summarised in Table 2 as showing

449     the respective coefficient of correlation (r), root mean square error (RMSE) and bias between

450     the data sets. Compared to SIM, the ERS-Scat data set has the highest overall correlation (r =

451     0.728) and lowest RMSE (0.201), followed by AMSR-E (VUA-NASA) with an r = 0.491 and

452     an RMSE of 0.297. As mentioned before, AMSR-E (NSIDC) has a negative correlation of –

453     0.014 with an RMSE of 0.370. The RMSE presented here is the RMSE obtained from the

454     normalised results, ie. it represents the relative error of the soil moisture dynamical range.

455     Assuming an average dynamic range of 0.3 $m^3m^{-3}$ and that SIM gives accurate in-situ

456     observations, this would translate into an average error of 0.056 $m^3m^{-3}$ for ERS-Scat, which is

457     higher than the design accuracy of SMOS (0.04 $m^3m^{-3}$).

458     Like the bias between the SIM and SMOSREX data sets, the biases shown between SIM

459     and the three satellite products are all positive. This suggests that a consistent dry bias exists

460     within SIM. A first explanation for the bias between SIM and SMOSREX are the different

461     thickness of the observed soil layers (1cm in the model against 0-6cm in-situ), as the deeper

462     profile of the in-situ observations is likely to maintain a higher soil moisture content, as it is

463     less affected by evaporation than the thin surface layer in the model. Furthermore, other

464     aspects such as erroneous soil type information, biased forcing data, and biases in the soil

465     moisture retrieval for the satellites may result in consistent biases.

466          *b. Correlations Specific to Land Surface Cover*

467          A comparison of vegetation maps with the results of Fig. 3 suggested a connection

468     between the accuracy of the remotely sensed soil moisture information and the land cover.

469     Therefore, the dominant land surface cover within each satellite-type pixel was determined,

470     using the information from ECOCLIMAP, in order to identify vegetation specific correlations

471     for each data product. For this purpose, the different vegetation types within each 0.25° pixel

472     were aggregated into three dominant cover types: i) cultivated soils, ii) grasslands, and iii)

473     forests (Fig. 4). Relatively good correlations exist between SIM, ERS-Scat and AMSR-E

474     (VUA-NASA) for the two herbaceous vegetation covers (Fig. 5a & b). Like in the analysis of

475     the overall data set, ERS-Scat and SIM have the highest correlation coefficient and lowest

476     RMSE. Similarly, the pairs SIM/AMSR-E (VUA-NASA) and AMSR-E (VUA-NASA)/ERS-

477     Scat have slightly lower correlation coefficients and higher RMSEs, and AMSR-E (NSIDC)

478     having negative correlations throughout. These results (with the exception of the AMSR-E

479     (NSIDC) data) are not surprising given that remotely sensed soil moisture information should

480     theoretically be retrievable with a high level of accuracy over herbaceous vegetation types. In

481     herbaceous vegetation covers, active and passive methodologies are expected to show similar

482     performances, especially when using a similar frequency. The higher correlations of ERS-

483     Scat and SIM as compared to AMSR-E (VUA-NASA) and SIM, shows potential for

484     improvement of the AMSR-E (VUA-NASA) product. Part of the difference might be

485     explained by the limited range of moisture values in the optimization routine for the AMSR-E

486     (VUA-NASA) product (0-50%). For the retrieval of the current AMSR-E (VUA-NASA) data,

487    the soil moisture content is limited to a maximum of 0.5 $m^3 m^{-3}$. However, it was found that

488    the surface soil moisture states often reached this point of saturation (Fig. 1). Consequently, if

489    this constraint were to be relaxed, and the retrieval process were allowed to produce higher

490    values, a quasi-normalised soil moisture product may be obtained (this aspect has been

491    considered for the next version of soil moisture data, which has recently been made

492    available). However, as a consequence of this constraint, the maximum soil moisture is

493    currently underestimated, which leads to an underestimation of the dynamic range, and

494    consequently a wet bias in the AMSR-E (VUA-NASA) data. The methodology behind the

495    ERS product avoids this caveat, by scaling between minimum and maximum observed signal

496    over the period 1992-2000.

497    The comparison of the various data sets for forested regions (Fig. 5c) overall shows lower

498    correlations and higher RMSEs. Again, ERS-Scat produces the best correlation with SIM,

499    followed by AMSR-E (VUA-NASA) and AMSR-E (NSIDC). Moreover, the ERS-Scat soil

500    moisture product appears to conserve its good correlation with SIM from the analysis of the

501    herbaceous vegetation types. Under the assumption that SIM is equally valid for forested

502    regions as for regions with low vegetation, it may be concluded that two effects may influence

503    the consistency of ERS-Scat for different vegetation types. Firstly, the retrieval process of

504    ERS-Scat implicitly takes into consideration the vegetation type by scaling the current signal

505    between the wet end dry ends of its long-term data base. This statement has significance for

506    other soil moisture missions in both active and passive microwave remote sensing, as the

507    approach taken for the retrieval of ERS-Scat soil moisture may be applied along with more

508    sophisticated radiative transfer models. Secondly, the ERS-Scat is well calibrated and has a

509    low radiometric noise of about 0.15 dB, which allows estimating soil moisture even in areas

510    where abundant forest cover reduces the effective sensitivity of backscatter to soil moisture.

511    An aspect of the data visible within the scatterplots of Fig. 5 is the apparent bi-modality

512    of the SIM data with data clouds forming for the lower and upper value ranges. Fig. 6 and 7

513    show histograms of the surface soil moisture from the four different low-resolution data

514    sources (SIM, AMSR-E (VUA-NASA), AMSR-E (NSIDC), and ERS-Scat) for SMOSREX

515    and for the whole of France, respectively. The histograms of the various data sources show

516    different patterns at the local scale (Fig. 6). While SIM and ERS-Scat show clear bi-

517    modalities, this is not the case for the two AMSR-E products, with AMSR-E (VUA-NASA)

518    having several peaks with a saturation at 1, and AMSR-E (NSIDC) data being almost

519    normally distributed, though all data sets, have a minima in the range of 0.4 to 0.6. The

520    histogram of the in-situ data at SMOSREX (Fig. 6e) also shows a bi-modality, although with

521    its maximum in the wet spectrum. This would suggest that preferred soil moisture states exist

522    at SMOSREX, but that the distribution is not correctly captured by the various models.

523    The non-normal distribution of the histograms have significance for the normalisation

524    process, as it was previously assumed that the soil moisture distribution was sufficiently

525    normal at each point. A violation of the assumption of normality would mean that the 90%

526    confidence interval could not be calculated with the equations (1) and (2). To assess this, the

527    distribution of the soil moisture states at the national scale was studied (Fig. 7).

528    An exception here is SIM with a clear peak in the dry spectrum (0.2) and AMSR-E

529    (VUA-NASA) being skewed towards the wet end (Fig. 7). The overall distributions show that

530    SIM retains its clear bi-modality with a peak in the dry spectrum, while the ERS-Scat and

531    AMSR-E data become more normally distributed. For the AMSR-E data sets, the distribution

532    of AMSR-E (NSIDC) data becomes almost Gaussian with a slight skew towards the wet end,

533    while the AMSR-E (VUA-NASA) data is more evenly distributed. As the normalisation

534    procedure of Pellarin et al. (2006) is only applied to the AMSR-E data, it is concluded that the

535    normalisation process is still applicable to the majority of the pixels throughout France.

536　　　The results shown here are in line with other studies. For example, Teuling et al. (2005)

537　　showed that preferred soil moisture states may exist locally. However, they found that this

538　　effect could not be observed at all sites studied and that it could not be linked to local soil

539　　conditions and may therefore be a random effect. This conclusion is supported by Fig. 6 and

540　　7, where the histograms for the data at SMOSREX suggest that local preferred wet and dry

541　　states exist, while the distribution of all observations over France is not bimodal.

542　　　　*c. Intra-seasonal Correlation*

543　　　The bi-modality presented in the previous section is unlikely to be caused by differences

544　　in the soil types, as the soil moisture data were normalised, and SMOSREX also appears to

545　　have this distribution (Fig. 6e). The bi-modality is related to the varying soil moisture states,

546　　which are caused by either precipitation events or seasons. As the effect of precipitation

547　　events on the soil moisture distribution is difficult to obtain, the results obtained for the

548　　cultivated soils in Fig. 5 were separated according to the various seasons. This analysis (Fig.

549　　8) clearly shows the different preferred soil moisture states in summer (dry) and winter (wet),

550　　which are consequently the main reason for the creation of the data clouds in Fig. 5. Similar

551　　results of preferred soil moisture states during the various seasons has been shown by Settin et

552　　al. (2007), where they were largely attributed to the precipitation intervals and intensities

553　　during the various seasons. Interestingly, the two AMSR-E products have nearly the same

554　　correlations with SIM during springtime, which would suggest that the two radiative transfer

555　　models work similarly well during this period.

556

557

558　**5. Conclusion**

559      In this paper, an intercomparison study of several remotely sensed surface soil moisture

560    products with the re-analysis LSM predictions over France has been presented. First, the LSM

561    predictions, and the satellite observations were compared with a 3-year in-situ surface soil

562    moisture data set from an experimental site in south-western France (SMOSREX) to

563    determine their capability to represent the temporal dynamics of a point or pixel. A good

564    correlation was found between the model predictions and the in-situ data, despite a slight dry

565    bias within the model predictions. Based on this evaluation, it was then assumed that the land

566    surface model predictions over France may be used as a credible approximate estimate in the

567    absence of more direct surface soil moisture observations for the whole country.

568      The analyses of this study, have shown that two of the three satellite data sets (AMSR-E

569    (VUA-NASA) and ERS-Scat) have generally a good correlation with the model predictions,

570    while the AMSR-E (NSIDC) data set did not correlate well with any of the other data sets.

571    Generally, the AMSR-E (NSIDC) data showed a significant lack of seasonal soil moisture

572    dynamics, which was well captured by the other data sets. These results suggest that the

573    AMSR-E (NSIDC) data set is not correct, as three other independent models (a physically

574    based radiative transfer model, an empiric soil moisture retrieval scheme, and a land surface

575    model) show a good correlation with each other. This is further supported by the good

576    correlation between SIM, AMSR-E (VUA-NASA), ERS-Scat and the in-situ observations at

577    SMOSREX. It is possible that those three models are all wrong and coincidentally produce

578    the same results, though the comparison with SMOSREX suggest that this is not likely. The

579    results of the observations obtained from the scatterometer additionally highlights the

580    potential use of active microwave data sets, which will be continued by the MetOp ASCAT

581    observations.

582      The analysis of de-trended time series (monthly anomalies) of surface soil moisture over

583    the SMOSREX site shows that short term variations of SIM and all the satellite products

584 (included the NSIDC AMSR-E product) are meaningful. The significance is less for ERS-

585 Scat, which has a high sampling time.

586     For the moment it has to be acknowledged that there exists a good correlation between

587 some products for densely vegetated areas, but further studies are required to validate their

588 physical meaning or relevance. Given that the we present only the temporal dynamics in this

589 paper, it is interesting to learn that some satellite products appear to represent those dynamics

590 better than others, even for forested areas.

591     While in-situ observations averaged to the land surface model or remotely sensed pixel

592 scale may be better suited for the evaluation of both land surface or radiative transfer models,

593 these observations are still sparse and difficult to obtain. This study presents an alternative to

594 the use of in-situ observations for such large scale evaluations through the inter-comparison

595 of independent and apparently similar soil moisture estimates from different models.

596

597     Finally, the good correlations between point observations and the low resolution model

598 predictions and satellite observations also show the importance of single point observations

599 for the verification of LSM and remotely sensed soil moisture products. They also support the

600 need of the installation of new and the maintenance of existing soil moisture monitoring

601 networks. This is particularly true for forested and mountainous regions, which in the past

602 have been neglected when new soil moisture monitoring sites were established. With the need

603 for the evaluation of land surface model performances and satellite validation campaigns, the

604 relatively few existing networks are not sufficient.

605

606

607 **Acknowledgments**

617

618

References

Boone, A., J.-C. Calvet, and J. Noilhan, 1999: Inclusion of a third soil layer in a land-surface scheme using the force-restore method, *J. Appl. Meteorol.*, **38**, 1611-1630.

Bartalis, Z., W. Wagner, V. Naeimi, S. Hasenauer, K. Scipal, H. Bonekamp, J. Figa, and C. Anderson, 2007: Initial soil moisture retrievals from the METOP-A Advanced Scatterometer (ASCAT). *Geophys. Res. Lett.*, **34**, L20401, 10.1029/2007GL031088

Bosch, D.D., V. Lakshmi, T.J. Jackson, M. Choi, and J.M. Jacobs, 2006: Large scale measurements of soil moisture for validation of remotely sensed data: Georgia soil moisture experiment of 2003. *J. Hydrol.*, **323**, 120-137.

Calvet, J.-C., J. Noilhan, and P. Bessemoulin, 1998a: Retrieving the root-zone soil moisture from surface soil moisture or temperature estimates: a feasibility study based on field measurements, *J. Appl. Meteorol.*, **37**, 371-386.

Calvet, J.-C., J. Noilhan, J.-L. Roujean, P. Bessemoulin, M. Cabelguenne, A. Olioso, and J.-P. Wigneron, 1998b: An interactive vegetation SVAT model tested against data from six contrasting sites, *Agr. For. Meteorol.*, **92**, 73-95.

Calvet, J.-C., P. Bessemoulin, J. Noilhan, C. Berne, I. Braud, et al., 1999: MUREX: a land-surface field experiment to study the annual cycle of the energy and water budgets, *Ann. Geophys.*, **17**, 838-854.

Calvet, J.-C., and J. Noilhan, 2000: From near-surface to root-zone soil moisture using year-round data, *J. Hydrometeorol.*, **1**, 393-411.

Calvet, J.-C., J. Muñoz Sabater, V. Vogt, J.-P. Wigneron, Y. Kerr, P. de Rosnay, C. Prigent, and T. Pellarin, 2005: Demonstration of the assimilation of the future SMOS data by using field and airborne campaigns. Abstracts volume, *Geophys. Res. Abstr.*, **7**, 04023, Sref-ID: 1607-7962/gra/EGU05-A-04023.

Cosh, M.H., T.J. Jackson, P. Starks, and G. Heathman, 2006: Temporal stability of surface soil moisture in the Little Washita River watershed and its applications in satellite soil moisture product validation. *J. Hydrol.*, **323**, 168-177.

De Rosnay, P., et al., 2006: SMOSREX: A long term field campaign experiment for soil moisture and land surface processes remote sensing. *Remote Sens. Environ.*, **102**, 377-389, doi:10.1016/j.rse.2006.02.021.

Dirmeyer, P. A., A. J. Dolman, and N. Sato, 1999: The Global Soil Wetness Project: A pilot project for global land surface modeling and validation. *Bull. Am. Meteorol. Soc.*, **80**, 851-878.

Draper, C.S., J.P. Walker, P.J. Steinle, R.A.M. de Jeu, and T.R.H. Holmes, 2007: Remotely sensed soil moisture over Australia from AMSR-E. Proceedings, *MODSIM 2007 International Congress on Modelling and Simulation*, Christchurch, New Zealand, Modelling and Simulation Society of Australia and New Zealand, in press.

Georgakakos, K.P., and T.M. Carpenter, 2006: Potential value of operationally available and spatially distributed ensemble soil water estimates for agriculture. *J. Hydrol.*, **328**, 177-191.

Grayson, R.B., and A.W. Western, 1998: Towards areal estimation of soil water content from point measurements: time and space stability of mean response. *J. Hydrol.*, **207**, 68-82.

Habets, F., A. Boone, J.L. Champeaux, P. Etchevers, L. Franchistéguy et al., 2008: The SAFRAN-ISBA-MODCOU hydrometeorological model applied over France. *J. Geophys. Res.*, 113, D06113, doi:10.1029/2007JD008548.

Kerr, Y.H., P. Waldteufel, J.-P. Wigneron, J. Font, and M. Berger, 2001: Soil moisture retrieval from space: The Soil Moisture and Ocean Salinity (SMOS) mission. *Geosci. Remote Sens.*, **39 (8)**, 1729-1735.

Li, L., E.G. Njoku, E. Im, P.S. Chang, and K. St. Germain, 2004: A preliminary survey of radio-frequency interference over the U.S. in Aqua AMSR-E data. *Geosci. Remote Sens.*, **42 (2)**, 380-390.

Li, L., P.W. Gaiser, M.H. Bettenhausen, and W. Johnston, 2006: WindSat radio-frequency interference signature and its identification over land and ocean. *Geosci. Remote Sens.*, **44 (3)**, 530-539.

Mätzler, C., and A. Standley, 2000: Relief effects for passive microwave remote sensing. *Int. J. Remote Sensing*, **21**, 2403-2412.

Meesters, A.G.C.A., R.A.M. De Jeu, and M. Owe, 2005: Analytical derivation of the vegetation optical depth from the microwave polarization difference index, *Geosc. Remot. Sens. Lett.*, **2(2)**,121-123.

National Snow and Ice Data Center (NSIDC). AMSR-E Level 3 B03 data set. http://nsidc.org/data/amsre/ (last accessed 7 November 2007).

Njoku, E.G., Jackson, T.J., Lakshmi, V., Chan, T.K., and S.V. Nghiem, 2003: Soil moisture retrieval from AMSR-E. *Geosci. Remote Sens.*, **41 (2)**, 215-229.

Noilhan, J., and S. Planton, 1989: A simple parameterization of land surface processes for meteorological models. *Mon. Wea. Rev.*, **117**, 536-549.

Noilhan, J., and J.-F. Mahfouf, 1996: The ISBA land surface parameterization scheme, *Global Planet. Change*, **13**, 145-159.

Owe, M., R. de Jeu, and J. Walker, 2001: A methodology for surface soil moisture and vegetation optical depth retrieval using the Microwave Polarisation Difference Index. *Geosci. Remote Sens.*, **39 (8)**, 1643-1654.

Owe, M., R. de Jeu, and T. Holmes, 2007: Multi-Sensor Historical Climatology of Satellite-Derived Global Land Surface Moisture, *J. Geophys. Res.*, doi:10.1029/2007JF000769, in press.

Pellarin, T., J.-C. Calvet, and W. Wagner, 2006: Evaluation of ERS scatterometer soil moisture products over a half-degree region in southwestern France. *Geosc. Remot. Sens. Lett.*, **33**, L17401, doi:10.1029/2006GL027231.

Prigent, C., F. Aires, W. B. Rossow, and A. Robock, 2005: Sensitivity of satellite microwave and infrared observations to soil moisture at a global scale: Relationship of satellite observations to in situ soil moisture measurements, *J. Geophys. Res.*, **110**, D07110, doi:10.1029/2004JD005087.

Quintana-Seguí, P., P. Le Moigne, Y. Durand, E. Martin, F. Habets, et al., 2008: Analysis of near-surface atmospheric variables: validation of the SAFRAN analysis over France. *J. Appl. Meteorol. Climatol.*, **47**, 92-107, doi:10.1175/2007JAMC1636.1.

Robock, A., K.Y. Vinnikov, G. Srinivasan, J.K. Entin, S.E. Hollinger, N.A. Speranskaya, S. Liu, and A. Namkhai, 2000: The global soil moisture data bank. *Bull. Am. Meteorol. Soc.*, **81**, 1281–1299.

Rüdiger, C. et al., 2007: Goulburn River experimental catchment data set. *Water Resour. Res.*, **43**, W10403, doi:10.1029/2006WR005837.

Sabater, J.M., L. Jarlan, J.-C. Calvet, F. Bouyssel, and P. De Rosnay, 2007: From near-surface to root-zone soil moisture using different assimilation techniques, *J. Hydrometeorol.*, **8**, 194-206.

Settin, T., G. Botter, I. Rodriguez-Iturbe, and A. Rinaldo, 2007: Numerical studies on soil moisture distributions in heterogeneous catchments. *Water Resour. Res.*, **43**, W05425, doi:10.1029/2006WR005737.

Teuling, A.J., R. Uijlenhoet, and P.A Troch, 2005: On bimodality in warm season soil moisture observations. *Geophys. Res. Lett.*, **32**, L13402, doi:10.1029/2005GL023223.

Vauchaud, G., A. Passerat de Silans, A. Balabanis, and M. Vauclin, 1985: Temporal stability of spatially measured soil water probability density function. *Soil Sci. Soc. Am. J.*, **49**, 822-828

Wagner, W., G. Lemoine, M. Borgeaud, and H. Rott, 1999a: A study of vegetation cover effects on ERS scatterometer data. *Geosci. Remote Sens.*, **37 (2)**, 938-948.

Wagner, W., J. Noll, M. Borgeaud, and H. Rott, 1999b: Monitoring soil moisture over the Canadian prairies with the ERS scatterometer. *Geosci. Remote Sens.*, **37 (1)**, 206-216.

Wagner, W., V. Naeimi, K. Scipal, R. de Jeu, and J. Martínez-Fernández, 2007: Soil moisture from operational meteorological satellites. *Hydrogeol. J.*, **15**,121-131.

**Figures**

Figure 1. Time series plots (2003-2005) of the normalised values of the in-situ observations at SMOSREX (black lines) and the four surface soil moisture products, SIM, AMSR-E (NSIDC), AMSR-E (VUA), and ERS-Scat (+). The model predictions and satellite observations were obtained from respective low-resolution pixels covering SMOSREX.

Figure 2. Scatterplot of the normalised in-situ soil moisture observations at SMOSREX (vertical axis) with the four low-resolution data sets (SIM, AMSR-E (VUA), AMSR-E (NSIDC), and ERS-Scat) for the years 2003-2005. Darker regions show a higher density of data points.

Figure 3. Maps of the coefficient of correlation between the various soil moisture products (normalised values) over mainland France. The circles highlight the 6 major metropolitan areas of France.

Figure 4. Location of pixels with the different dominant land cover types (cultivated soils, grasslands, and forests), based on the fractional covers obtained from Ecoclimap and aggregated to 0.25° resolution.

Figure 5. Vegetation type specific comparison of the different soil moisture products for the three dominant vegetation types (a) cultivated soils, b) grasslands, c) forests), using the data from the period 2003-2005. The scatterplots and their corresponding statistics are located on opposite sides of each figure, ie. the scatterplot of the data pair SIM-AMSR (VUA) is in the

top left hand corner, while the respective statistical values are found in the bottom right hand corner. Darker regions show a higher density of data points.

Figure 6. Histograms showing the relative frequency (vertical axis) of the various normalised soil moisture observations (horizontal axis) and predictions for the years 2003-2005 for the SMOSREX site: SIM model, AMSR-E product of VUA-NASA, AMSR-E product of NSIDC, ERS-Scat product of University of Vienna, in situ observations.

Figure 7. Histograms showing the relative frequency (vertical axis) of the various normalised soil moisture observations (horizontal axis) and predictions for the years 2003-2005 for whole of France: SIM model, AMSR-E product of VUA-NASA, AMSR-E product of NSIDC, ERS-Scat product of University of Vienna.

Figure 8. Scatterplots showing the comparison of the various soil moisture products for pixels with herbaceous vegetation only (cultivated soils and grasslands) for the four seasons a) spring, b) summer, c) autumn, and d) winter. The scatterplots and their corresponding statistics are located on opposite sides of each figure, ie. the scatterplot of the data pair SIM-AMSR (VUA) is in the top left hand corner, while the respective statistical values are found in the bottom right hand corner. Darker regions show a higher density of data points.

**Tables**

Table 1 – Comparison of monthly anomalies of surface soil moisture products (SIM, AMSR-E, ERS-Scat) with in-situ 0-6cm observations at the SMOSREX site, for three pooled annual cycles (2003 to 2005).

| Product | Season | Number | Correlation | Bias | RMSE | Kendall $\tau$ | Kendall p-value |
|---|---|---|---|---|---|---|---|
| SIM | All | 794 | 0.61 | 0.01 | 0.79 | 0.63 | **** |
| SIM | DJF | 121 | 0.44 | -0.03 | 0.93 | 0.53 | ** |
| SIM | MAM | 219 | 0.74 | 0.01 | 0.65 | 0.73 | **** |
| SIM | JJA | 255 | 0.58 | 0.03 | 0.78 | 0.58 | **** |
| SIM | SON | 199 | 0.65 | 0.04 | 0.79 | 0.66 | **** |
| AMSR-E (NSIDC) | All | 698 | 0.46 | 0.01 | 0.88 | 0.39 | **** |
| AMSR-E (NSIDC) | DJF | 95 | 0.27 | -0.20 | 0.99 | 0.17 | NS |
| AMSR-E (NSIDC) | MAM | 192 | 0.62 | 0.11 | 0.77 | 0.54 | **** |
| AMSR-E (NSIDC) | JJA | 219 | 0.23 | 0.02 | 1.03 | 0.21 | ** |
| AMSR-E (NSIDC) | SON | 192 | 0.54 | 0.01 | 0.88 | 0.48 | **** |
| AMSR-E (VUA-NASA) | All | 606 | 0.38 | 0.01 | 0.97 | 0.38 | **** |
| AMSR-E (VUA-NASA) | DJF | 75 | 0.12 | -0.07 | 1.05 | 0.01 | NS |
| AMSR-E (VUA-NASA) | MAM | 172 | 0.49 | 0.09 | 0.90 | 0.53 | **** |
| AMSR-E (VUA-NASA) | JJA | 184 | 0.28 | 0.01 | 1.00 | 0.28 | *** |
| AMSR-E (VUA-NASA) | SON | 175 | 0.42 | 0.00 | 1.01 | 0.44 | **** |
| ERS-Scat | All | 133 | 0.34 | -0.08 | 0.85 | 0.30 | ** |
| ERS-Scat | DJF | 32 | 0.57 | -0.12 | 0.51 | 0.39 | NS |
| ERS-Scat | MAM | 32 | 0.55 | -0.06 | 0.54 | 0.57 | * |
| ERS-Scat | JJA | 28 | 0.28 | -0.10 | 0.64 | 0.30 | NS |
| ERS-Scat | SON | 41 | 0.19 | 0.02 | 0.81 | 0.07 | NS |

*The monthly anomaly is the difference to the mean divided by the standard deviation, for a period of 5 weeks. The Kendall $\tau$ is a non-parametric measure of correlation that assesses how well an arbitrary monotonic function could describe the relationship between two variables, without making any assumptions about the frequency distribution of the variables. It is used to measure the degree of correspondence between two rankings and assessing the significance of this correspondence. The p-value indicates the significance of the test, if it is small (below 0.05 at least), it means that the correlation is not a coincidence. The following thresholds on p-values are used: (i) NS (non significant) for p-value greater than 0.05, (ii) \* between 0.05 and 0.01, (iii) \*\* between 0.01 and 0.001, (iv) \*\*\* between 0.001 and 0.0001 and (v) \*\*\*\* below a value of 0.0001.*

Table 2 – Statistics of the inter-comparison between the difference data sets (normalised surface soil moisture data). The values in each cell correspond to the coefficient of correlation, bias, and RMSE, respectively.

| | | SIM | ERS-Scat | AMSR-E (VUA-NASA) |
|---|---|---|---|---|
| AMSR-E (NSIDC) | r<br>bias<br>RMSE | -0.014<br>0.215<br>0.370 | -0.099<br>0.040<br>0.363 | -0.115<br>0.043<br>0.361 |
| AMSR-E (VUA-NASA) | r<br>bias<br>RMSE | 0.491<br>0.177<br>0.297 | 0.397<br>0.099<br>0.296 | |
| ERS-Scat | r<br>bias<br>RMSE | 0.728<br>0.093<br>0.201 | | |

**Figures**

Fig. 1 Time series plots (2003-2005) of the normalised values of the in-situ observations at SMOSREX (black lines) and the four surface soil moisture products, SIM, AMSR-E (NSIDC), AMSR-E (VUA), and ERS-Scat (+). The model predictions and satellite observations were obtained from respective low-resolution pixels covering SMOSREX.
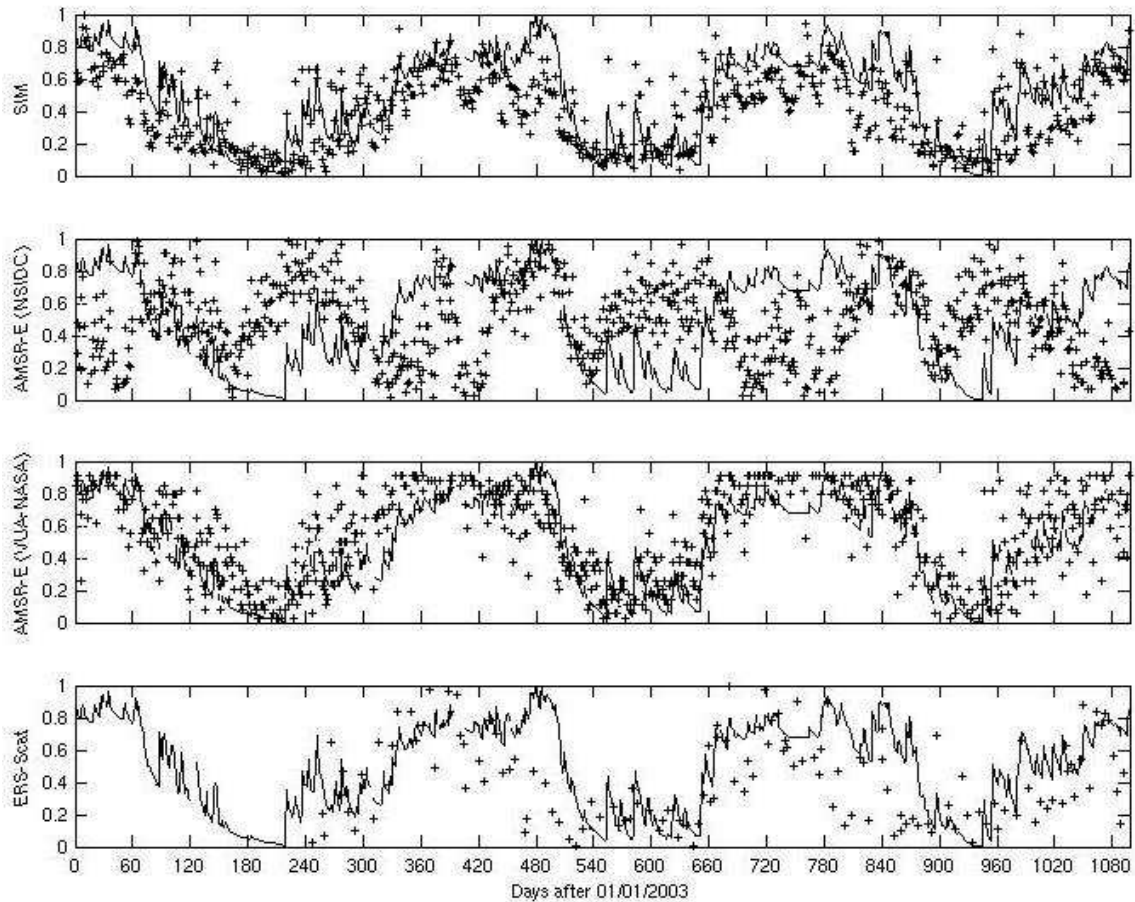
Fig. 2 Scatterplot of the normalised in-situ soil moisture observations at SMOSREX (vertical axis) with the four low-resolution data sets (SIM, AMSR-E (VUA), AMSR-E (NSIDC), and ERS-Scat) for the years 2003-2005. Darker regions show a higher density of data points.
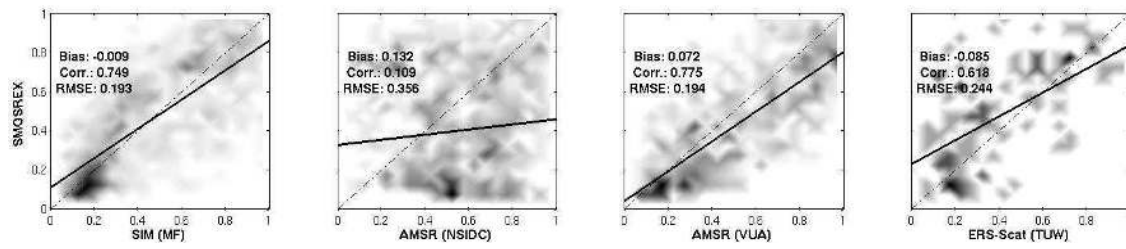
Fig. 3 Maps of the coefficient of correlation between the various soil moisture products (normalised values) over mainland France. The circles highlight the 6 major metropolitan areas of France.



Soil Moisture (Normalised) Correlation Maps for France, Years 2003-2005
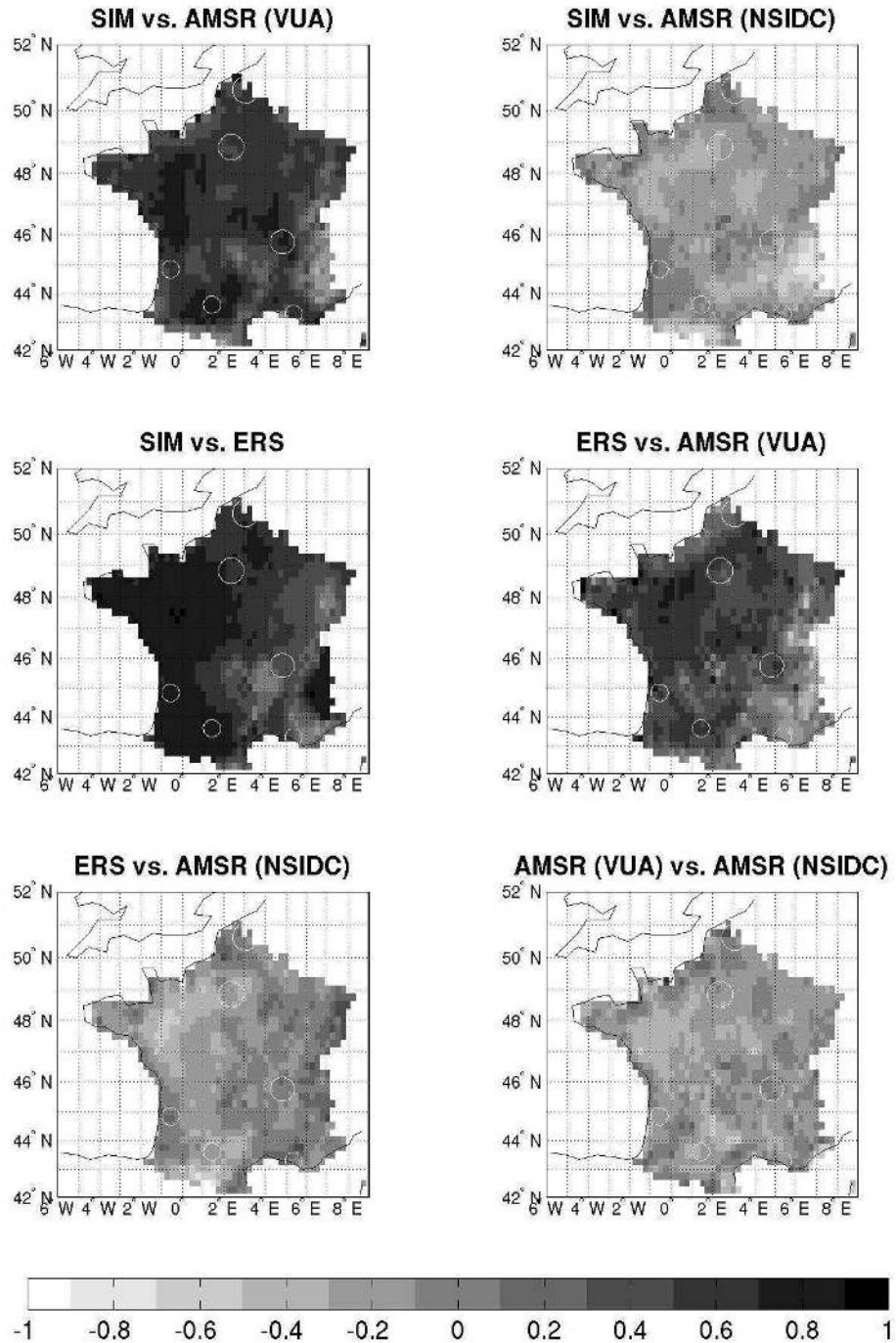
Fig. 4 Location of pixels with the different dominant land cover types (cultivated soils, grasslands, and forests), based on the fractional covers obtained from Ecoclimap and aggregated to 0.25° resolution.
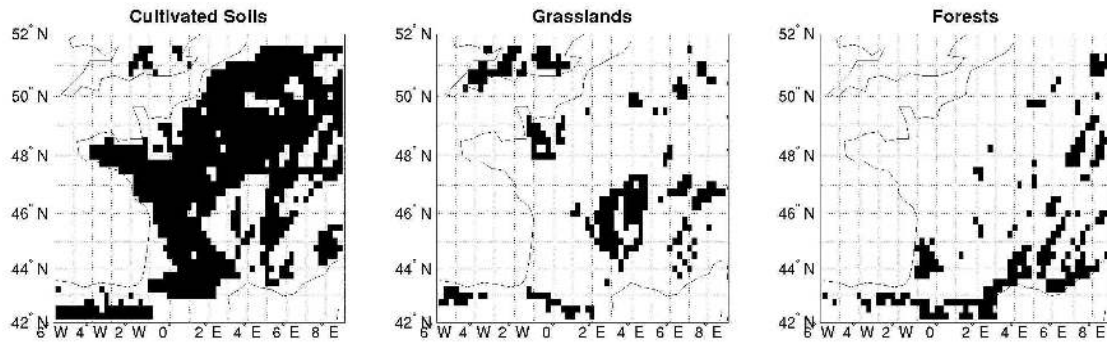
Fig. 5 Vegetation type specific comparison of the different soil moisture products for the three dominant vegetation types (a) cultivated soils, b) grasslands, c) forests), using the data from the period 2003-2005. The scatterplots and their corresponding statistics are located on opposite sides of each figure, ie. the scatterplot of the data pair SIM-AMSR (VUA) is in the top left hand corner, while the respective statistical values are found in the bottom right hand corner. Darker regions show a higher density of data points.
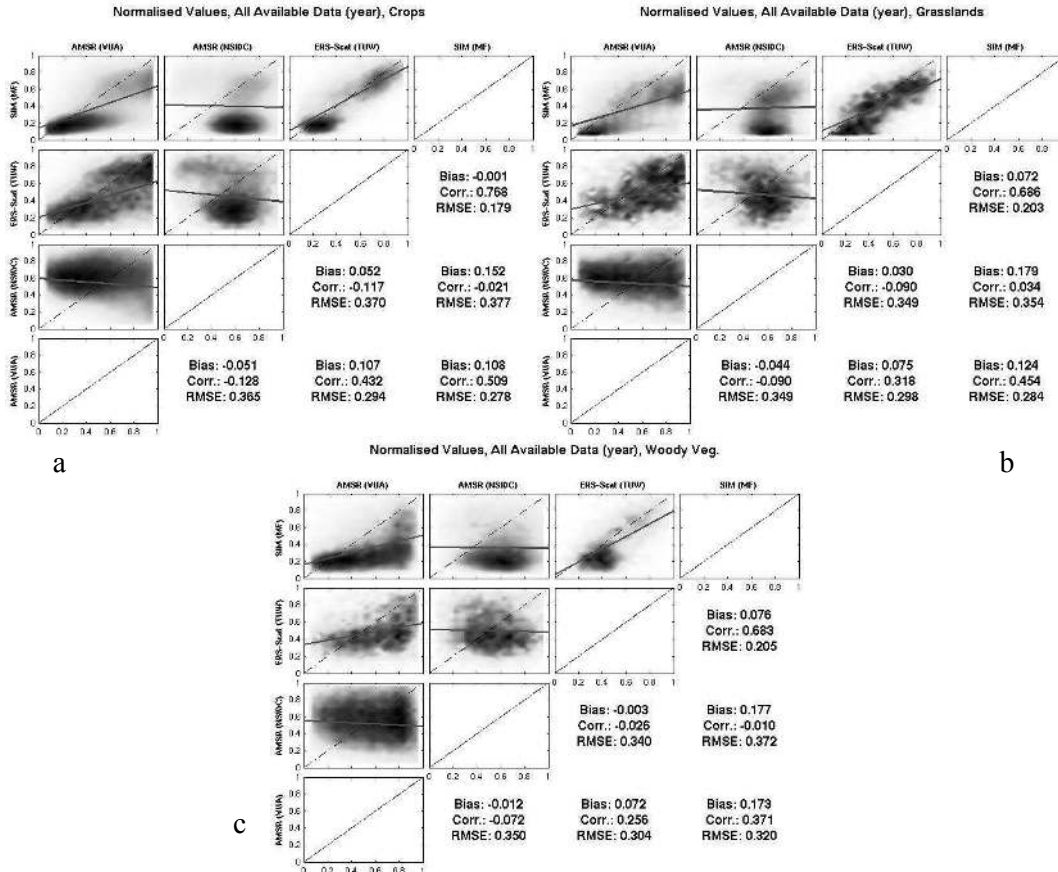


a

b

c

Fig 6. Histograms showing the relative frequency (vertical axis) of the various normalised soil moisture observations (horizontal axis) and predictions for the years 2003-2005 for the SMOSREX site: SIM model, AMSR-E product of VUA-NASA, AMSR-E product of NSIDC, ERS-Scat product of University of Vienna, in situ observations.
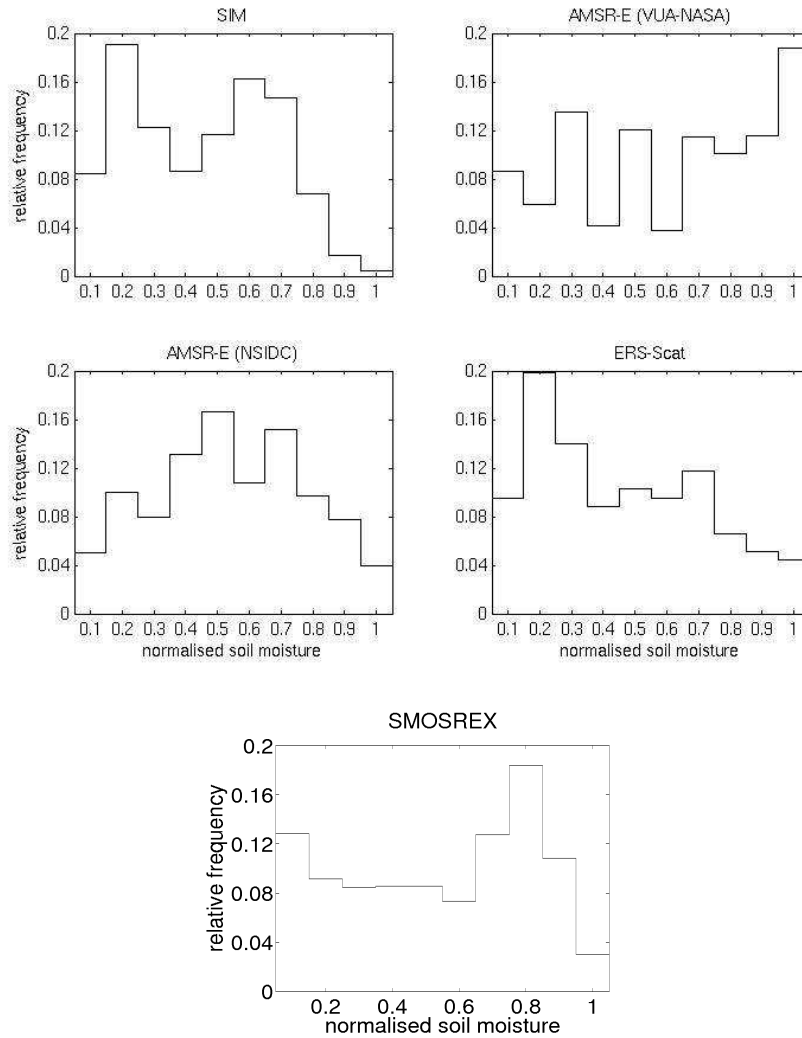
Fig 7. Histograms showing the relative frequency (vertical axis) of the various normalised soil moisture observations (horizontal axis) and predictions for the years 2003-2005 for whole of France: SIM model, AMSR-E product of VUA-NASA, AMSR-E product of NSIDC, ERS-Scat product of University of Vienna.
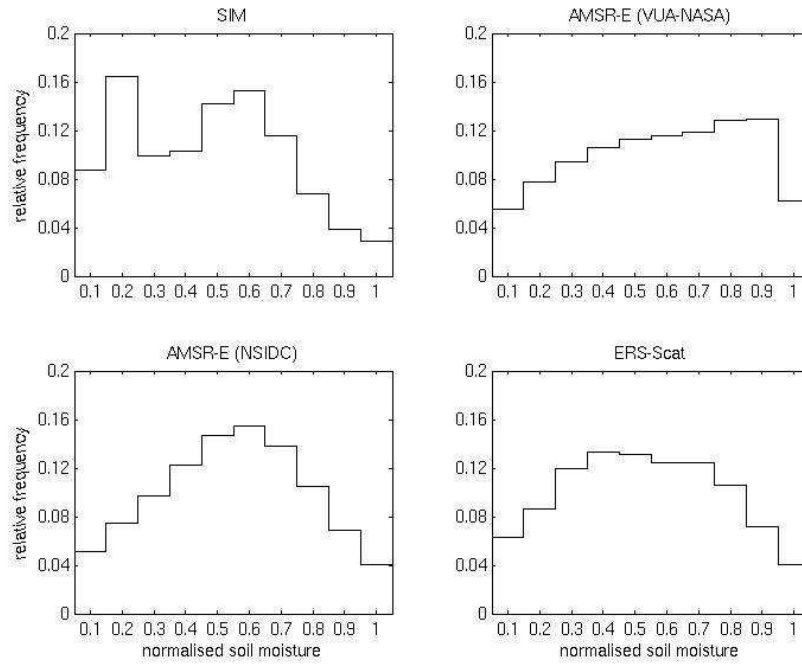
Fig. 8 Scatterplots showing the comparison of the various soil moisture products for pixels with herbaceous vegetation only (cultivated soils and grasslands) for the four seasons a) spring, b) summer, c) autumn, and d) winter. The scatterplots and their corresponding statistics are located on opposite sides of each figure, ie. the scatterplot of the data pair SIM-AMSR (VUA) is in the top left hand corner, while the respective statistical values are found in the bottom right hand corner. Darker regions show a higher density of data points.